Ecological Engineering 212 (2025) 107537

Contents lists available at ScienceDirect

Ecological Engineering

journal homepage: www.elsevier.com/locate/ecoleng

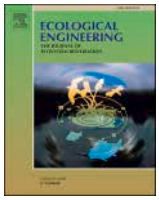

Soil erosion control in tree plantations on steep slopes: Runoff water and sediment trapping efficiency of riparian grass buffer in mountainous humid tropics

Layheang Song [a,b], Olivier Ribolzi [a,*], Laurie Boithias [a], Khampaseuth Xayyathip [c], Christian Valentin [d], Bounsamay Soulileuth [c], Henri Robain [d], Anneke de Rouw [d], Phabvilay Sounyafong [c], Norbert Silvera [c], Phimmasone Sisouvanh [e], Jean-Louis Janeau [d], Inpeng Saveng [f], Chantha Oeurng [b], Alain Pierret [a]

[a] GET, Université de Toulouse, CNRS, IRD, UPS, 31400 Toulouse, France
[b] Research and Innovation Center, Institute of Technology of Cambodia, Russian Federation Blvd, P.O. Box 86, Phnom Penh, Cambodia
[c] IRD, IEES-Paris UMR 242, c/o National Agriculture and Forestry Research Institute, Vientiane 01000, Laos
[d] Institute of Ecology and Environmental Sciences of Paris (iEES-Paris), Sorbonne Université, Univ Paris Est Creteil, IRD, CNRS, INRAe, 75005 Paris, France
[e] National University of Laos (NUoL), Faculty of Agriculture, Nabong Campus, Ban Paksap Mai, Xaythany District, Vientiane, Laos
[f] Department of Agricultural Land Management (DALaM), P.O. Box 4195, Ban Nogviengkham, Xaythany District, Vientiane 01000, Laos

ARTICLE INFO

Keywords:
Southeast Asia, Tropical agroecosystems, Soil loss mitigation, Nature-based solutions, Ecosystem services

ABSTRACT

Riparian grass buffers reduce the velocity of water flowing over the soil surface during storms, capturing surface runoff (SR) and trapping soil particles eroded from cultivated slopes. Rarely quantified under steep slope conditions (>45 %), this phenomenon probably occurs in many mountain agroecosystems in the humid tropics. In Southeast Asia, teak plantations are often established on steep slopes where they can lead to significant soil loss (SL), particularly when the understory is removed. Therefore, we aimed to: quantify the effect of riparian grass buffers on SR and SL downstream of a teak plantation; and estimate the trapping efficiency of riparian grass buffers for water (WTE) and sediment (STE). Field measurements were carried out in Northern Lao PDR during the2014 rainy season, considering riparian zones with contrasted ground covers: (1) uncovered (URZ - 7-year-old teak trees with mean grass and litter densities of 7 % (SD 2 %) and 4 % (SD 3 %), respectively; (2) transitional (TRZ - 7-year-old teak trees with mean grass and litter densities of 19 % (SD 10 %) and 56 % (SD 9 %), respectively; and (3) covered (CRZ - grassed areas without teak trees with mean grass and litter densities of 46 % (SD 13 %) and 47 % (SD 21 %), respectively). WTE and STE were estimated based on measurements carried out from 6 July to 6 September2014 under natural rainfall conditions, using pairs of triplicate Gerlach troughs installed at the upper and lower margins of 5- and 10-m riparian sections (encompassing areas of ~25 and 50 m^2, respectively). Runoff coefficient (Rc), SL, and soil surface features were measured on the occasion of 20 rainfall events in 1-m^2 microplots. Rc and SL were higher in URZ (56 %, 5791 $g{\cdot}m^{-2}$) than in TRZ (13 %, 250 $g{\cdot}m^{-2}$) and CRZ (19 %, 159 $g{\cdot}m^{-2}$). Median WTE and STE were the highest along the 10-m TRZ + CRZ riparian grass buffer at 85 % and 97 % respectively. Partial Least Square Regression (PLSR) modelling yielded a good agreement between observation and prediction for WTE and STE at seasonal scale. Overall, the results of this work indicate that 5 to 10 m riparian grass buffers limit the export of surface water and sediment downstream during small (24-h rainfall $\leq$20.9 $mm{\cdot}d^{-1}$, return period $\leq$1 year) to large storms (40.0 $mm{\cdot}d^{-1}$ < 24-h rainfall $\leq$84.5 $mm{\cdot}d^{-1}$, 1.01 year<return period$\leq$2 years).

1. Introduction

Globally, mechanical erosion of soil by water is a major cause of soil degradation, resulting from both natural processes and anthropogenic activities. Soil erosion has far-reaching economic, political, social and environmental implications (Pimentel, 2006) due to the loss of

* Corresponding author.
E-mail address: olivier.ribolzi@ird.fr (O. Ribolzi).

https://doi.org/10.1016/j.ecoleng.2025.107537
Received 31 July 2024; Received in revised form 17 December 2024; Accepted 21 January 2025
Available online 1 February 2025

ecosystem services (Sartori et al., 2019) as well as negative effects, both on- and off-site (Valentin and Rajot, 2018). On-site, main negative effects of soil erosion are soil quality and productivity reduction (Dregne, 1995), while off-site negative effects consist of downstream effects such as dam siltation (Wei et al., 2019) or stream water pollution (Boithias et al., 2021b). Soil erosion can be strongly aggravated by human-induced activities, particularly unsuitable agricultural practices (Perron et al., 2024; Wuepper et al., 2020). Common human-induced factors of soil erosion include deforestation, overgrazing, and intensive and extensive cultivation (Ahmad et al., 2020). In turn, soil erosion exacerbated by improper agricultural practices leads to crop productivity losses, which subsequently impact the economy and threaten food security (Sartori et al., 2019).

Because of sloping land, mountain areas are particularly prone to soil erosion (Ahmad et al., 2020; Bhat et al., 2019; Huon et al., 2017; Sharma et al., 2017). In addition, soil erosion is further enhanced by the tropical climates that prevail in the mountain areas of Southeast Asia (Borrelli et al., 2017), with heavy storms often triggering the delivery of large amounts of suspended sediment to streams (Sidle et al., 2006). To mitigate soil erosion on agricultural land, Ahmad et al. (2020) drew up an inventory of management control practices such as tillage operation techniques, intercropping, ground cover crop, mulching, organic matter management, and grass cultivation.

It is widely accepted among planners and policy makers that reforestation is an effective means to mitigate soil erosion and rehabilitate degraded land (Calder et al., 2004; Sanz et al., 2017). However, this consensus needs to be qualified because it is well documented that certain types of tree cover with large leafed species, such as teak (*Tectona grandis),* can lead to significant soil loss (Calder, 2001). Likewise, the hydrological behaviour and the susceptibility to erosion of afforested agroecosystems can be radically different depending on management and whether it is planted or naturally regenerated (Lacombe et al., 2016; Miyata et al., 2009; van Meerveld et al., 2021; Wiersum, 1985; Xaysatith et al., 2022). For example, in northern Lao PDR, it was found that the switch from shifting cultivation to teak plantations resulted in a 6-fold increase in soil loss (Ribolzi et al., 2017). In the same geographical area, Song et al. (2020) found that maintaining understorey vegetation in teak plantations mitigated surface runoff and soil loss.

Riparian buffer conservation policies are absent or poorly defined in most tropical countries and while recent reports such as Luke et al. (2019) indicate that the protection of narrow buffers (c. 5–10 m) could be a means of regulating hydrology in tropical farmland, it is also recognised that catchment characteristics such as road layout or forest cover structure can outweigh the impact of localised riparian buffers. Previous investigations in tropical hillslopes also demonstrated that the sediment trapping efficiency of dense grass riparian buffers was influenced by slope morphology, understory vegetation density and flow channelisation in highly convergent catchments (McKergow et al., 2004a). Further, it was also reported that while all runoff infiltrated into riparian soil during small rainfall events, infiltration was in contrast limited during large events which are characteristic of wet tropical conditions (McKergow et al., 2004b).

Given the problems of soil loss in some tree plantations, especially in mountainous areas of Southeast Asia (Neyret et al., 2020), maintaining grass buffer zones in riparian areas is likely important for erosion control (Vigiak et al., 2008). Grassed buffer zones are also reportedly effective in trapping surface runoff and eroded soil particles in a variety of agro-ecosystems (Alemu et al., 2017; Bereswill et al., 2014; Dong et al., 2018; Gumiere et al., 2011; Mekonnen et al., 2014; Pan et al., 2018) and may contribute to conserving downstream water quality (Angelsen and Kaimowitz, 2004; Cao et al., 2018; Ding et al., 2011; Dosskey et al., 2010; Vidon and Hill, 2004). However, the trapping efficiency of riparian buffer zones depends on their width (Castelle et al., 1994), which can vary from a few meters to a few hundreds of meters, and is highly site-specific. Based on modelling, Ziegler et al. (2006) found that 17 to 47 m buffer zones trap surface runoff with an efficiency of 65 to 85 % in fragmented landscapes of northern Vietnam. They suggested keeping riparian buffer zones as wide as possible to maximize trapping efficiencies during more severe storms. However, it can be anticipated that maintaining or creating riparian buffer zones of several tens of metres is hardly acceptable to farmers in the context of Southeast Asian uplands (Lestrelin and Giordano, 2007). In teak plantations of Northern Lao PDR (Boithias et al., 2021a), most of the plots are planted right up to the edge of the stream (de Rouw et al., 2018) and where a buffer zone is maintained, its width, which rarely exceeds 10 m, is at most 25 m.

Given the potential of riparian buffer zones for trapping hydro-sedimentary flows in humid tropical mountain agro-ecosystems (Vigiak et al., 2008), and considering the severity of erosion problems in some tropical tree plantations (Neyret et al., 2020; Ribolzi et al., 2017), the aim of this study was to test two hypotheses relating to the effectiveness of narrow (10 m wide at most) riparian buffer zone conservation as a means of mitigating soil loss and sediment export in the context of mountain agroecosystems in northern Laos. The novelty of this work was to carry out this assessment of the effectiveness of riparian grass buffer strips in catchments where teak tree plantations, known to generate very high runoff and soil loss (Ribolzi et al., 2017) are predominant and where hillslopes are steep (>50 % on average).

The first hypothesis tested was that bio-physical characteristics of riparian grass buffer zones such as grass and litter cover densities and soil surface features, increase soil hydraulic conductivity while reducing overland flow velocity, thus reducing soil detachment and soil transfer downslope.

The second hypothesis was that riparian grass buffer zones 5 to 10 m wide, which are socially acceptable dimensions for upland farmers in northern Laos, can act as effective sediment traps and thus help to improve water quality in streams and reduce sediment exports.

To test these hypotheses, microplots (Patin et al., 2018) and Gerlach troughs (Comino et al., 2016; Kagabo et al., 2013; Thomaz, 2009; Vigiak et al., 2008), were deployed in a riparian area downstream from a teak tree plantation in three adjacent subplots varying in grass and litter cover densities. Microplots are bounded devices that allow to quantify runoff coefficient and soil loss at the very local scale but from which no inference can be made about sediment trapping (since no inflow runoff is measured). Gerlach traps, on the other hand, are used to quantify sediment tapping at the slope scale. This experimental setup was used to measure an array of soil, hydro-sedimentary and surface feature descriptors rarely taken into account in studies dealing with the sediment trapping performance of riparian vegetation strips.

2. Materials and methods

2.1. Study area

The experimental site was located about 10 km from Luang Prabang in Northern Lao PDR (Fig. 1), on the left bank of the Houay Pano stream, in the Southeastern part of the Houay Pano headwater catchment (Boithias et al., 2021a). This catchment is part of the Multiscale TROPIcal CatchmentS network of critical zone observatories (M-TROPICS CZO; https://mtropics.obs-mip.fr/). It is representative of Southeast Asian montane agro-ecosystems undergoing conversion from shifting cultivation to commercial tree plantations (Ribolzi et al., 2017). Altitudes within the catchment range from 435 to 716 m a.s.l. with an average slope gradient of 52 % (range: 1–135 %). Soils within the catchment are Entisol, Ultisol and Alfisol (USDA Soil Taxonomy). In the early 2000s, ~80 % of the land was farmed in rotation, while ~50 % were planted in teak trees in the early 2020s (Boithias et al., 2021a, 2021b). The climate is sub-tropical humid and is characterized by a monsoon regime with a dry season from November to May, and a rainy season from June to October. The mean annual rainfall is 1366 mm, 71 % falling during the rainy season (rainfall measured from 2001 to 2019 using an automatic rain gauge located ~300 m North of the study site – Fig. 1a). The mean annual temperature is 23.4 °C.

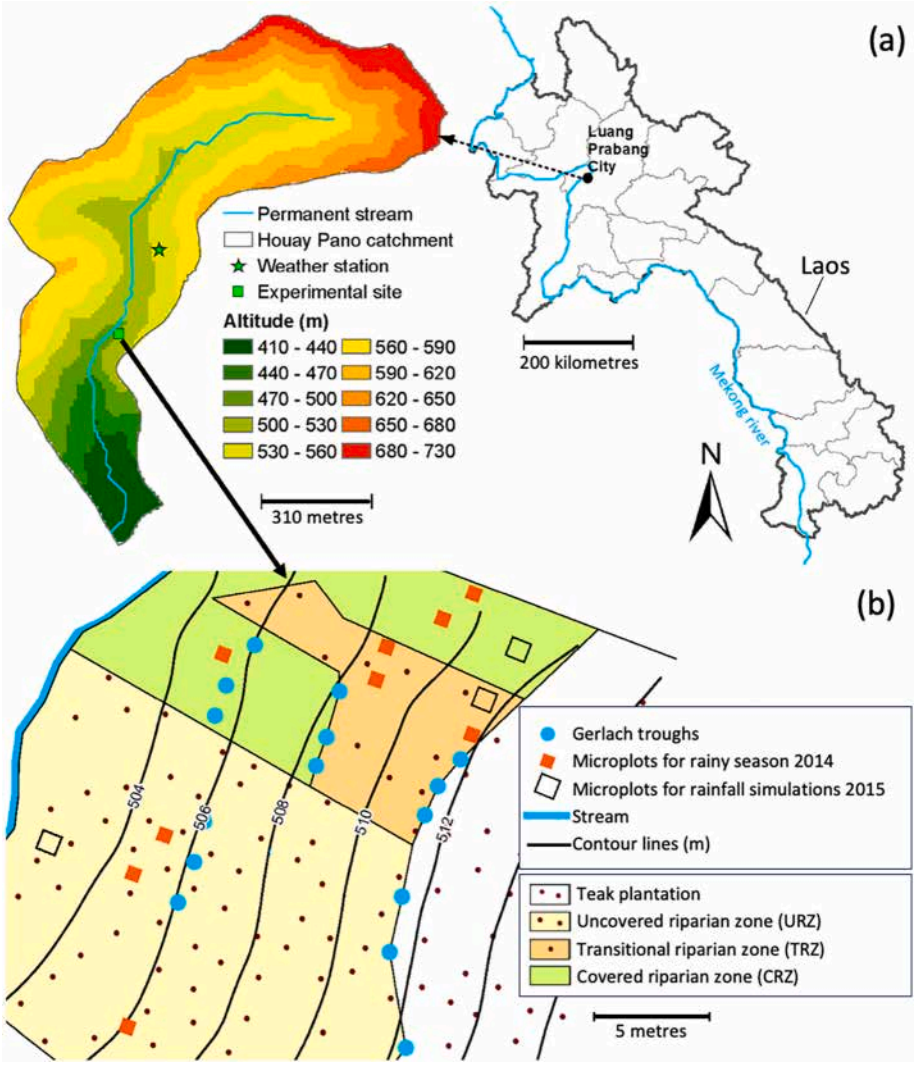

Fig. 1. Location and configuration of the experimental site. Location (a) of the Houay Pano catchment in northern Lao PDR, and of the riparian experimental site within the catchment. (b) Positioning of 1-m^2 microplots used during the rainy season in Bu et al., 2014 and for rainfall simulations in 2015; 0.5-m Gerlach troughs during the rainy season of Bu et al., 2014; mapping of the uphill teak plantation and of the riparian zone situations (i.e., covered, transition and uncovered).

2.2. Experimental design

The experiment was conducted during the Bu et al., 2014 rainy season, from 6 July to 22 September, on a plot of approximately 30 × 30 m in the riparian zone of the Houay Pano stream, downhill from a teak tree plantation with fully leafy canopy (Fig. 1). Within this plot, riparian zone types with contrasted ground cover conditions (Fig. A.1) were considered, namely:

- "uncovered riparian zone" (URZ) at the downhill edge of a 7-year-old teak plantation (Fig. 2a), where the soil surface has very sparse or no litter cover (mean 4 %, SD 3 %) and grass cover (mean 7 %, SD 2 %);
- "transitional riparian zone" (TRZ) with 7-year-old teak trees (Fig. 2b) and with soil covered by litter (mean 56 %, SD 9 %) and grass (mean 19 %, SD 10 %);
- "covered riparian zone" (CRZ) without teak trees (Fig. 2b), with soil surface equally covered by litter (mean 47 %, SD 21 %) and grass (mean 46 %, SD 13 %).

In this experiment, the grass cover consisted of *Microstegium ciliatum* (Trinius) *A. Camus*, a local perennial grass growing in dense masses, creeping in its lower part and rooting at the nodes.

Two types of devices were deployed in the different types of riparian zones (Fig. 1b), and were sampled on the same dates, namely: 1. microplots (Fig. 2e) which were used to assess runoff coefficient, soil detachment (as a function of incident throughfall) and to characterise soil surface features and 2. Gerlach troughs (Fig. 2f) which were used as tools to determine water and sediment overland flows and derive trapping efficiencies.

The criterion used to decide to carry out sampling was the presence of run-off water in the Gerlach troughs and in the microplot collecting buckets following rainfall events that generally had a maximum peak intensity and a cumulative depth of at least 15 $mm \cdot h^{-1}$ and 10 mm, respectively (Fig. A.2). During the study period, samples were taken on 20 and 19 dates with microplots and Gerlach troughs, respectively, as Gerlach troughs had not yet been installed when event E_1 occurred.

For ease of reading, the meaning of the abbreviations of variables and descriptors used in the article is given in Table A.1.

2.3. Rainfall measurements and rainfall-related indices

Rainfall was measured at 6-min intervals as part of the long-term M-TROPICS monitoring (Boithias et al., 2021a). In order to analyze and interpret the records from microplots and Gerlach troughs in relation to rainfall, weather station data were used to calculate rainfall indices described in the next two paragraphs.

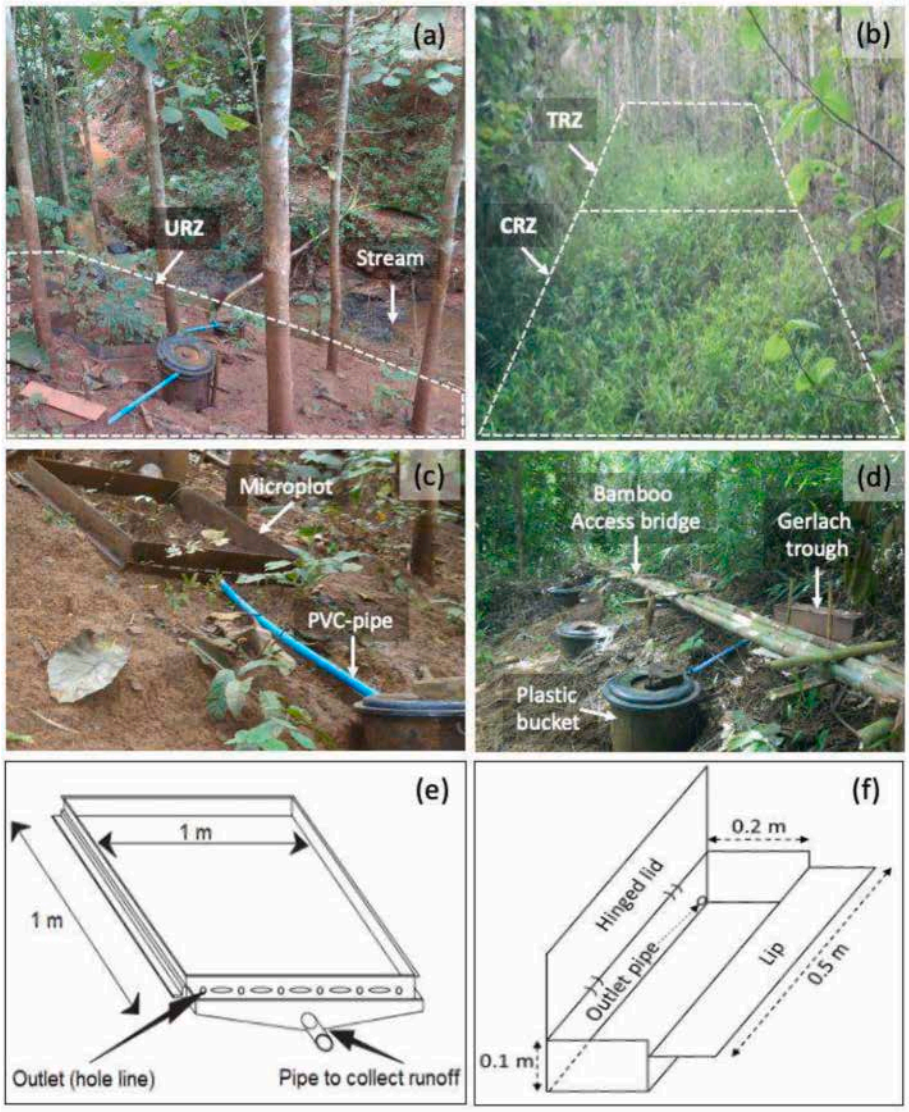

Fig. 2. Main features and field deployment of microplot and Gerlach troughs. Experimental setup: (a) downward view of the stream from the "uncovered riparian zone" (URZ) with 7-year-old teaks; (b) upward view from the stream, of the "transitional riparian zone" (TRZ) with grass cover and 7-year-old teaks, and of the "covered riparian zone" (CRZ) with grass cover; (c) picture of a microplot in the URZ; (d) picture of three Gerlach troughs along the lower rim of the CRZ; and schematic of (e) a microplot and (f) a Gerlach trough.

2.3.1. Rainfall depths indices

Four rainfall depth indices were defined as follows:

- rainfall depth preceding each rainfall event (see dotted grey lines in Fig. A.2) that triggered surface runoff and sampling (Sign_R, mm);
- cumulative rainfall depth corresponding to a 24-h period prior to a sampling date (24_R, mm);
- cumulative rainfall depth (see black lines in Fig. A.2) between two sampling dates (Acc_R, mm);
- seasonal rainfall depth calculated by summing up Acc_R values corresponding to the experiment duration ($Rain_{SEAS}$, mm).

2.3.2. Return period of maximum daily rainfall

The representativeness of the 20 rainfall events monitored in Bu et al., 2014 was assessed by classifying them according to their 24_R value into four categories defined as follows (Table A.2): small (S), medium (M), large (L), and exceptional (E) daily rainfall with $S < 20.9$ $mm.d^{-1} < M < 40.0$ $mm.d^{-1} < L < 84.5$ $mm.d^{-1} < E$.

2.3.3. Rainfall kinetic energy indices

Rainfall kinetic energy (KE, $J{\cdot}m^{-2}$) was computed as suggested by Kinnell (1981) and Van Dijk et al. (2002), using the following equation:

$$e_k = e_{kmax}(1 - a \bullet exp(-b \bullet I)) \quad (1)$$

$$KE = \Sigma(e_k \bullet I \bullet \Delta t) \quad (2)$$

Where e_k is the rainfall kinetic energy content ($J{\cdot}mm^{-1}{\cdot}m^{-2}$), e_{kmax} is the maximum energy content ($J{\cdot}mm^{-1}{\cdot}m^{-2}$), a (−) and b ($h{\cdot}mm^{-1}$) are empirical constants, I is rainfall intensity ($mm{\cdot}h^{-1}$) and the sum Σ is computed over discrete time intervals. The effect of different tree canopy structures on KE (Lacombe et al., 2018) was accounted for by using a, b, and e_{kmax} estimates extracted from Patin et al. (2018). Values of $a = 0.66 \pm 0.04$, $b = 0.02 \pm 0.01$, $e_{kmax} = 28.4 \pm 4.3$ were thus selected for CRZ (KE_o, $J{\cdot}m^{-2}$) while values of $a = 0.70 \pm 0.18$, $b = 0.23 \pm 0.09$, $e_{kmax} = 33.5 \pm 1.6$ were used for TRZ and URZ (KE_t, $J{\cdot}m^{-2}$).

Two indices related to rainfall kinetic energies were estimated:

- cumulative rainfall kinetic energy between two sampling dates (Acc_KE, $J{\cdot}m^{-2}$);

- seasonal rainfall kinetic energy calculated by summing up Acc_KE values corresponding to the experiment duration (KE_{SEAS}, $J{\cdot}m^{-2}$).

The Erosivity Index (EI30, $MJ{\cdot}mm{\cdot}ha^{-1}{\cdot}h^{-1}$) was computed using *KE* and maximum 30-min rainfall intensity (I30, $mm{\cdot}h^{-1}$) using the following equation:

$$EI30 = KE \bullet I30 \quad (3)$$

We calculated erosivity indices for CRZ as EI30_o ($MJ{\cdot}mm{\cdot}ha^{-1}{\cdot}h^{-1}$) and for TRZ and URZ as EI30_t ($MJ{\cdot}mm{\cdot}ha^{-1}{\cdot}h^{-1}$) using KE_o and KE_t, respectively, for each Sign_R.

2.4. Biophysical characterization of riparian zone soil

2.4.1. Microplot assessment of runoff and soil loss

Surface runoff (SR, mm) and soil loss (SL, $g{\cdot}m^{-2}$) were monitored following an approach similar to that of Patin et al. (2018). Triplicate microplots were installed in URZ, TRZ and CRZ (Fig. 1b). Microplots consist of 1-m^2 metal frames with 0.15-m high edges (Fig. 2e) inserted into the soil and connected by a plastic pipe to a ~ 40-l plastic bucket (Fig. 2c). Runoff water and sediment were sampled from the buckets using 650-mL plastic bottles. Samples were collected after thoroughly stirring the water in the bucket until the suspended sediment was homogenously distributed within the water column. The water volume and suspended sediment accumulated in the bucket after sampling using a plastic measuring beaker were also measured. After each sample collection, the buckets were emptied.

The runoff coefficient (Rc, %) was calculated as the ratio in percentage between SR and Acc_R. Seasonal surface runoff (SR_{SEAS}, mm) during the experiment was also calculated by summing up the SR of the 20 samplings. The seasonal runoff coefficient (Rc_{SEAS}, %) over the whole rainy season was calculated as the ratio between SR_{SEAS} and $Rain_{SEAS}$.

Sediment mass of each sample was measured following flocculation, filtration and oven dehydration of the water samples. The suspended sediment concentration (SSC, $g{\cdot}L^{-1}$) was calculated as the ratio between the sediment mass and the volume of the sample. SL, i.e. the total weight of suspended sediment in the bucket, was calculated by multiplying SSC by the total volume of runoff water collected in the bucket. The soil loss over the whole rainy season (SL_{SEAS}) was estimated by cumulating suspended sediment mass corresponding to the 20 samplings.

2.4.2. Saturated hydraulic conductivity

The saturated hydraulic conductivity of the soil (K, $mm{\cdot}h^{-1}$) was measured at the surface of URZ, TRZ and CRZ using a field rainfall simulator with raindrop size distribution and kinetic energy similar to those of tropical rainfall (Ribolzi et al., 2011). Rainfall simulations were carried out in March 2015 on three 1-m^2 microplots (Le et al., 2020), each one installed in one of the riparian zone types (Fig. 1b). K was obtained from the steady-state infiltration rate obtained at the end of the simulation, when the soil surface was saturated, by subtracting the runoff intensity from the rainfall intensity (Foltz et al., 2009).

2.4.3. Soil physical properties

Soil physical properties of the top soil layer in the 3 riparian zone types were measured at a depth of 7.5 cm using 5-cm-high standard 100-cm^3 cylinders. Average values were obtained from 6 replicates. The three texture classes (i.e., Clay 2 μm; Silt 2–50 μm; Sand 50–2000 μm) were determined by the standard pipette method from the fraction lower than 2 mm.

2.4.4. Grass cover and soil surface features assessment

Areal percentage of grass cover and soil surface features were assessed by visual inspection in each replicate microplot at the beginning (14 June) and in the middle (27 August) of the2014 rainy season based on the method proposed by Casenave and Valentin (1992). Surface features included the areal percentages of grass (Gra, %), litter (Lit, %; leaves, branches, seeds), worm casts (Wor, %; constructions by soil macro-organisms like earthworms), mosses (Mos, %), algae (Alg, %), charcoals (Cha, %), free aggregates (Fa, %), free gravel (Fg, %), pedestals (Ped, %), and total crust (Tc, %) (Fig. A.4.). For each riparian zone situations (i.e. URZ, TRZ and CRZ), grand means of the percentages of each surface feature observed on two occasions in triplicate microplots were used for subsequent analysis (Fig. 1).

2.5. Surface runoff and sediment trapping efficiencies

Surface runoff and sediment trapping efficiencies of URZ, TRZ and CRZ were estimated using fifteen 0.5-m Gerlach troughs (Gerlach, 1967) connected by a PVC tube to a plastic bucket (Fig. 2d and f) following Vigiak et al. (2008).

To monitor the incoming and outgoing surface runoff, Gerlach troughs were deployed in triplicate at the upper and lower margins of two plots, one encompassing TRZ + CRZ and the other one URZ, each extending 10-m in the direction of the steepest slope. For the TRZ + CRZ plot, an additional triplet of Gerlach troughs was positioned mid-plot in order to be able to estimate both the flow leaving TRZ and entering CRZ. Small bridges made of bamboo were installed alongside the troughs in order to access them without disturbing the ground surface (Fig. 2d). To summarize, based on this experimental set-up, fifteen Gerlach troughs were deployed to define combinations of four riparian zones as follows:

- TRZ + CRZ corresponding to the 10 m wide slope with TRZ uphill and CRZ downhill
- TRZ corresponding to the 5 m wide uphill half of TRZ + CRZ
- CRZ corresponding to 5 m wide downhill half of TRZ + CRZ
- URZ corresponding to 10 m wide slope in URZ

2.5.1. Surface runoff and suspended sediment

To calculate surface runoff water (Run, $L{\cdot}m^{-1}$), we multiplied the volume of water measured in the Gerlach trough buckets by two in order to normalize the incoming surface runoff for a linear distance of 1 m. As for microplots, suspended sediment concentration (Con, $g{\cdot}L^{-1}$) was estimated from a water sample taken using 650-mL plastic bottles. The total weight of suspended sediment in the bucket, i.e., Sed, ($g{\cdot}m^{-1}$), was then calculated by multiplying Con by Run. We calculated the seasonal volume of surface runoff (Run_{SEAS}) and the seasonal weight of sediment (Sed_{SEAS}) by summing up Run and Sed, respectively, of all the 19 events. Seasonal sediment concentration (Con_{SEAS}) was calculated by dividing Sed_{SEAS} by Run_{SEAS}.

2.5.2. Water and sediment trapping efficiencies

For each of the 19 events, trapping efficiency (TE, dimensionless) of riparian zones was calculated for surface runoff water (WTE, dimensionless) and sediment (STE, dimensionless) following McKergow et al. (2004):

$$TE = (X_{in} - X_{out})/X_{in} \quad (5)$$

where X_{in} is Run for WTE or Sed for STE of the upper Gerlach trough (inflow), and X_{out} is Run for WTE or Sed for STE of the lower Gerlach trough (outflow).

We calculated WTE and STE for each four combinations of riparian zones listed above (i.e. TRZ + CRZ, TRZ, CRZ and URZ). We also calculated seasonal WTE (WTE_{SEAS}) and seasonal STE (STE_{SEAS}) using Run_{SEAS} and Sed_{SEAS}, respectively.

2.6. Descriptive statistics and modelling

Statistical analyses were conducted using XLSTAT version 20.4.1 (Addinsoft., 2021). Spearman's rank correlation coefficients and significance levels (p-value <0.05) were estimated to test the statistical

relationship between both Rc_{SEAS} and SL_{SEAS}, and the areal percentage of soil surface features measured in the microplots (Table A.3). The non-parametric Kruskal-Wallis test (p-value <0.05) was applied to compare the distributions of surface runoff, suspended sediment concentration and runoff coefficient values pooled for each set of triplicate microplots installed in the URZ, TRZ and CRZ riparian zone types because the values of these distributions were non-normal and there were more than two independent groups to compare. Similarly and for the same data conditions, the Kruskal-Wallis test was applied to compare the distributions of water and sediment trapping efficiencies (WTE and STE) derived from Gerlach trough measurements.

2.6.1. Partial Least Square Regression (PLSR)

We applied Partial Least Square Regression (PLSR) (Abdi, 2010) to model WTE_{SEAS} and STE_{SEAS}. We selected this approach as it is well suited to situations where the number of explanatory variables exceeds the number of observations, and with collinearities between some of these variables. In our case, the number of observations was four, corresponding to the four combinations of riparian zones listed above (i.e., TRZ + CRZ, TRZ, CRZ and URZ), while the number of variables was 15 and included: rainfall characteristics ($Rain_{SEAS}$ and KE_{SEAS}); areal percentages of the main soil surface features measured (Fa, Fg, Tc, Res, Wor, Ped, and Gra); topographical conditions such as slope (Slope) and width of the riparian zone (Width); hydraulic properties of soil surface (K, Rc_{SEAS}); and the seasonal characteristics of the upstream surface runoff flow entering the riparian zone in terms of volume (Run_{SEAS_up}) and sediment concentration (Con_{SEAS_up}). Variables with Variable Importance in the Projection (VIP) scores above the empirical threshold of 0.8 were considered the best predictors in the models (Wold, 1995).

2.6.2. Soil loss model

In an effort to explain the variance of SL (SSC x SR) measurements obtained using microplots, we applied a soil erosion model proposed by Patin et al. (2018), corresponding to an adaptation of the TEST model (Van Dijk et al., 200; Van Dijk and Bruijnzed; 2004a,b), originally developed to analyze runoff and soil loss in terrace systems under natural rainfall. TEST describes rainfall-driven transport by splash and shallow overland flow as a function of vegetation and soil surface cover. It was adapted to the specific conditions of the steep hillslopes by Patin et al. (2018) and applied at the plot and annual scales. This model is calibrated using percentages of vegetation and litter at the ground surface as well as sediment yields for sufficient rainfall events. The model is expressed as:

$$SL = D \bullet \Sigma(KE \cdot Rc) \bullet \exp.(-a \bullet Gra) \bullet \exp.(-b \bullet Lit).$$

where SL is the soil loss on the microplot scale ($g \bullet m^{-2}$), D is the effective soil detachability ($g \cdot J^{-1}$); KE is the rainfall kinetic energy ($J \cdot m^{-2}$); Rc is the runoff coefficient (%); Gra is the areal percentage of grass (%); Lit is the areal percentage of litter (%); a and b are the decay coefficients of Gra and Lit, respectively.

3. Results

All the data measured in this article are available on a public repository (Ribolzi et al., 2024).

3.1. Vegetation cover and soil characteristics

URZ, TRZ and CRZ displayed similar top soil physical properties with clay texture (USDA classification) in the three riparian zone types and average bulk densities ranging from 1.06 to 1.12 g cm^{-3} (Table. A.5). The three zones displayed contrasting tree, grass and litter areal cover percentages (Fig. A.1), as well as contrasted soil surface features (Fig. A.3) and soil saturated hydraulic conductivity:

- CRZ had no tree cover while in URZ and TRZ the tree areal cover was 92 % and 33 %, respectively (average tree height: 8 m and 2.2 m, respectively);
- URZ had an average grass areal cover of 7 % while in CRZ, the soil was densely covered by *Microstegium ciliatum* (45 % areal cover), and grass leaves had an average height of 0.78 m;
- The areal coverages of some soil surface features were similar in CRZ and TRZ (Fig. A.3): total crusts (2 %); free aggregates (40–50 %); and litter (47–56 %). In URZ, total crusts reached 90 %, free aggregates were 6 % and litter 4 %. Structural crust accounted for 100 % of the total crusts in CRZ and TRZ and for 81 % in URZ. The average height of pedestal features varied from 0.5 to 4 cm in CRZ and URZ, respectively. The areal percentage of pedestal features was 73.8 and 0.5 % in URZ, TRZ and CRZ, respectively;
- Median surface K values were 23, 86 and 72 $mm \cdot h^{-1}$, in URZ, CRZ and TRZ, respectively.

3.2. Rainfall, rainfall kinetic energy, and erosivity

The2014 cumulative rainfall was 1365 mm, of which 863 mm (63 %) occurred during the sampling period. 24_R exceeded 30 $mm \cdot d^{-1}$ for eight rainfall events, Sign_R and Acc_R exceeded 30 and 50 mm for six rainfall events, respectively. I30 was greater than 20 $mm \cdot h^{-1}$ for eight rainfall events (Table A.4). KE_o and KE_t exceeded 400 $J \cdot m^{-2}$ for seven and ten rainfall events, respectively. EI30_o and EI30_t exceeded 100 $MJ \cdot mm \cdot ha^{-1} \cdot h^{-1}$ for seven and nine rainfall events, respectively. Seven events had a 24_R value lower than 20.9 $mm \cdot d^{-1}$ ($R = 1$ year), hence classified as minor (events 1, 2, 3, 9, 10, 11, and 17). Eight events were classified as medium (events 4, 7, 8, 12, 13, 14, 16 and 20) with a 24_R value between 20.9 and 40 $mm \cdot d^{-1}$. Four events which had a 24_R value between 40 and 84.5 $mm \cdot d^{-1}$ were classified as large (events 5, 6, 15 and 18). The highest 24_R value measured (189.4 $mm \cdot d^{-1}$), which corresponds to a return period of more than hundred years ($R = 109$ years), was observed for the event 19, which was classified as exceptional.

3.3. Surface runoff and soil loss measurements using microplots

Fig. 3 provides an overview of the distribution of surface runoff and sediment measurements at the event scale in URZ, TRZ and CRZ: SR was significantly higher (p-value <0.05) in URZ than in TRZ and CRZ; SSC and Rc were also significantly higher in URZ (p-value <0.05) than in TRZ and CRZ. SSC was significantly lower in CRZ than in TRZ (p-value <0.05) (Fig. 3b).

After calibration and validation, the model of Patin et al. (2018), including observations from the three types of riparain zones, explained more than 90 % of the variance in SL and revealed the importance of Rc, KE, Gra and Lit in sediment production in the riparian zone of the catchment (see fig. A.4). This figure shows observed and the modelled soil loss at the event scale. The model performance was $R^2 = 0.91$ for calibration and 0.92 for validation (p-value <0.001).

Fig. 4 shows the relationship between Rc_{SEAS} and SL_{SEAS} for all microplots. Given the wide range of SL_{SEAS} values (93–6548 $g \cdot m^{-2}$), these have been plotted on a logarithmic scale. Indeed, very high seasonal accumulations of soil loss are observed for URZ (4425–6548 $g \cdot m^{-2}$) compared with the other two types of riparian zones TRZ and CRZ, whose values appeared up to more than one order of magnitude lower, and within a more limited range (93–480 $g \cdot m^{-2}$). Average SL_{SEAS} were 5791, 250 and 159 $g \cdot m^{-2}$ in URZ, TRZ and CRZ, respectively, giving an overall average of 2067 $g \cdot m^{-2}$ for all riparian zones combined. Rc_{SEAS} shows a similar contrast between URZ, whose values are high and exceed 50 % (54–68 %), compared with TRZ and URZ, having values below 30 % (7–25 %). Average Rc_{SEAS} over the experimental period were 55, 13, and 19 % in URZ, TRZ, and CRZ, respectively.

The average SR_{SEAS} from microplot triplicates was 4.5 and 3 times higher in URZ (415 mm) compared to TRZ (93 mm) and CRZ (138 mm),

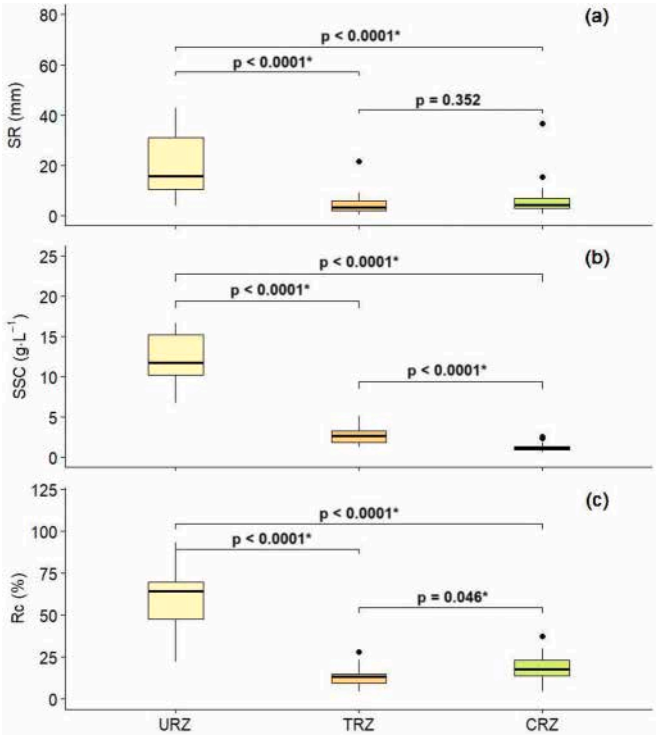

Fig. 3. Distributions of surface runoff, suspended sediment concentration and runoff coefficient values pooled for each set of triplicate microplots installed in the URZ, TRZ and CRZ riparian zone types. Boxplots of (a) surface runoff (SR), (b) suspended sediment concentration (SSC), and (c) runoff coefficient (Rc) measurements using the 9 microplots installed in the riparian zone types (i.e., URZ: uncovered riparian zone; TRZ: transitional riparian zone; CRZ: covered riparian zone) and for the 20 rainfall events sampled between 6 July and 22 September Bu et al., 2014. For each boxplot, the central horizontal line is the median value, the upper and lower box hinges are the 25th and 75th percentiles, and the whiskers extend 1.5× the spread of the hinges. Data points outside the whiskers are outliers, indicated by black dots. *P*-values of Kruskal-Wallis tests are indicated above horizontal lines linking compared pairs of boxplots.

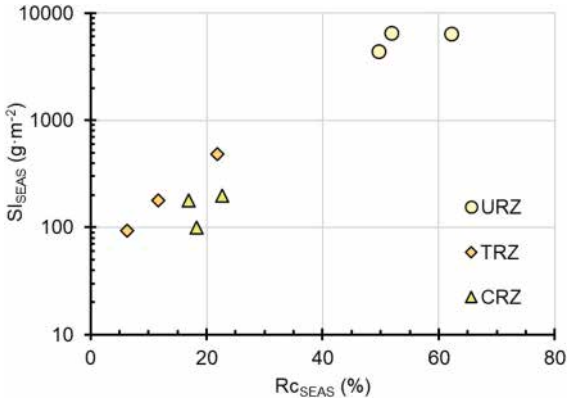

Fig. 4. Relationship between seasonal runoff coefficient (Rc_{SEAS}, %) and seasonal soil loss (SL_{SEAS}, $g \cdot m^{-2}$, logarithmic scale) measurements using the 9 microplots installed in the 3 riparian zone types (i.e., URZ: uncovered riparian zone; TRZ: transitional riparian zone; CRZ: covered riparian zone).

respectively. The average Rc_{SEAS} for URZ, CRZ, and TRZ were 55 %, 19 %, and 13 %, respectively. At 5791 $g \cdot m^{-2}$, URZ also had the highest average SL_{SEAS} value, 23 and 36 times that in TRZ (250 $g \cdot m^{-2}$) and CRZ (159 $g \cdot m^{-2}$), respectively.

Spearman's correlation coefficients were calculated in order to assess the link between Rc_{SEAS} and SL_{SEAS} with the main soil surface features observed on microplots (Table A.3). Res and Wor were negatively correlated with Rc_{SEAS} ($r = -0.88$ and $r = -0.83$, respectively). Although strongly correlated to Rc_{SEAS} ($r = 0.92$), SL_{SEAS} appeared significantly correlated with a greater number of observed variables than Rc_{SEAS}: it is positively correlated with Tc ($r = 0.80$) and Ped ($r = 0.73$). SL_{SEAS} is also negatively correlated with Gra ($r = -0.73$) and, like Rc, also negatively correlated with Res ($r = -074$) and Wor ($r = -0.85$). Soil surface features were correlated with each other except for Fg, Alg and Mos.

3.4. Surface runoff and suspended sediment observations using Gerlach troughs

Fig. 5 shows the double mass curves for Run and Sed as a function of Acc_R. The Run and Sed values are the average measured at the four main Gerlach trough rims (Fig. 1b): downstream of CRZ; downstream of TRZ; downstream of URZ; and upstream URZ, i.e., the Run and Sed values of the surface runoff from the teak plantation upstream of the study area. For Run, the figure shows distinct linear relationships (Fig. 5a), with slope ranking CRZ (0.137 ± 0.04) < TRZ (0.50 ± 0.02) < Teak plantation (0.82 ± 0.01) < URZ (1.27 ± 0.02). For Sed, the ranking of the curves is similar to that of Run, but they follow non-linear patterns (Fig. 5b), particularly "Teak plantation" and URZ which, after an initial phase of rapid increase up to about 250 mm cumulative rainfall, shows a slowdown.

Cumulative Run were at most 135 $L \cdot m^{-1}$ and 484 $L \cdot m^{-1}$, while cumulative Sed were 1.3 $kg \cdot m^{-1}$ and 6.4 and $kg \cdot m^{-1}$, downstream of CRZ and TRZ, respectively, therefore much lower than at the downstream

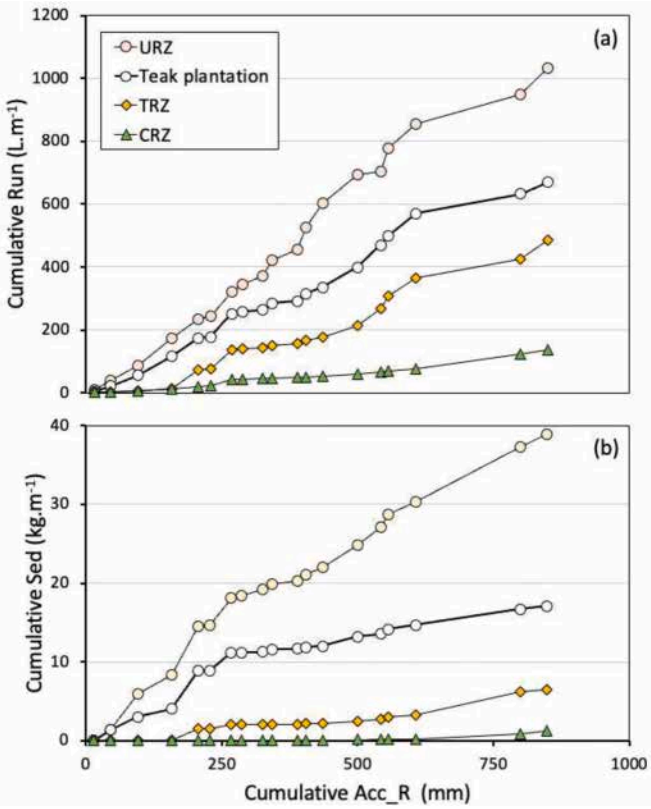

Fig. 5. Cumulative curves of (a) surface runoff volume per unit of length (Run) and of (b) sediment weight per unit of length as a function of cumulative rainwater depth (Acc_R). Run and Sed values are averages of the measurements from the Gerlach trough located at the lower rim of the uncovered riparian zone (URZ), of the transitional riparian zone (TRZ), of the covered riparian zone (CRZ) and at the upper rim of the riparian zone, i.e., downhill of the teak plantation (Teak plantation) upstream of the study area.

edge of the teak plantation (i.e., upper boundary of the study area), where they reached 669 $L{\cdot}m^{-1}$ and 17.1 $kg{\cdot}m^{-1}$. On the contrary, the values measured downstream of URZ were higher than at the downstream edge of the teak plantation, reaching 1032 $L{\cdot}m^{-1}$ and 38.8 $kg{\cdot}m^{-1}$, respectively, for Run and Sed.

Ranking of WTE_{SEAS} and STE_{SEAS} for the four riparian zone types was URZ < TRZ < CRZ < TRZ + CRZ (Fig. 6). WTE_{SEAS} and STE_{SEAS} are positive for TRZ, CRZ and CRZ + TRZ, with values close to 0.3 for TRZ, about 0.7 for CRZ, and just over 0.8 for TRZ + CRZ. On the other hand, values for URZ are negative at −0.68 and − 0.78, for WTE_{SEAS} and STE_{SEAS}, respectively.

Fig. 7 shows all the WTE and STE values measured in the four riparian zone types and for the 19 rainfall events. The distributions of WTE and STE values for the four treatments all appear significantly different from one another (p-value <0.05) with the sole exception of WTE between TRZ and CRZ. In all cases, the treatments TRZ, CRZ and TRZ + CRZ differed very strongly from URZ (p-value <0.001). The median WTE and STE values for the four riparian zones show rankings in line with the cumulative seasonal values described above (Fig. 6): URZ < TRZ < CRZ < TRZ + CRZ. Over the monitoring period, URZ values were predominantly negative, with only one and two events showing positive values for WTE and STE respectively. In contrast, WTE and STE were predominantly positive in the other zones with grass cover (i.e. TRZ, CRZ and TRZ + CRZ). There were only two negative STE values for TRZ, and four and two negative WTE values for TRZ and CRZ, respectively. The range of WTE and STE values differed from one zone to another: it was the highest for URZ, with an interquartile range of 0.93 and 1.03 for WTE and STE, respectively, compared with TRZ + CRZ which, by contrast, displayed very low dispersion of values, with interquartiles of 0.06 and 0.01 for WTE and STE, respectively. Fig. 7 reveals that, at the rainfall event scale, WTE and STE are independent of rainfall intensity. Only the exceptional event of 17 September (number 19, red dots on the figure) shows systematically low values for STE, as well as for WTE, with the exception of URZ. In the latter case, due to the high intensity and cumulative rainfall depth values (Table A.4), Gerlach troughs were overflowed, and the WTE and STE values were therefore biased.

3.5. Analysis of water and sediment trapping efficiency using the PLSR

The previous paragraph shows that the intensity of the rainfall event does not explain the distribution of WTE and STE values. In this section, the PLSR analysis includes a larger number of explanatory variables (i.e., 15) in an attempt to explain the WTE_{SEAS} and STE_{SEAS} values (Fig. 8a).

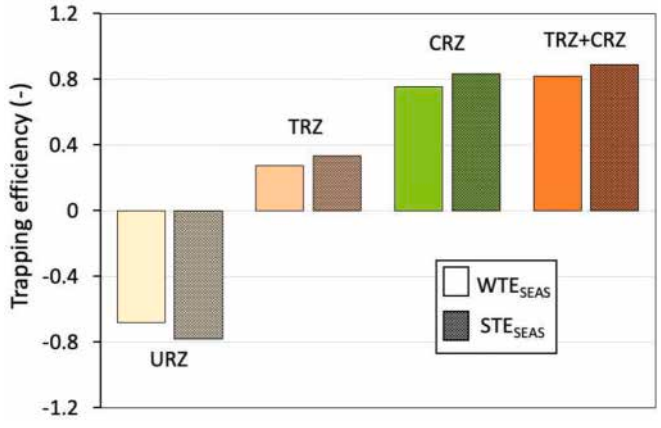

Fig. 6. Seasonal trapping efficiency for water (WTE_{SEAS}) and sediment (STE_{SEAS}) for the four riparian zone types (i.e. URZ: 10 m wide uncovered riparian zone; TRZ: 5 m wide transitional riparian zone; CRZ: 5 m wide covered riparian zone; TRZ + CRZ: 10 m wide slope with TRZ uphill and CRZ downhill) measured between 6 July and 22 September2014.

The sum of the determination coefficients between the dependent variables and the first two components is 0.98, which indicates a very good explanatory power of the first plan with respect to WTE_{SEAS} and STE_{SEAS}. Similarly, the model has good predictive power with respect to the explanatory variables with, in this case, a sum of the determination coefficients of 0.95. It can be seen that WTE_{SEAS} and STE_{SEAS} are very close to each other, and appear positively correlated to K and Fa and to a lesser extent to Wor, Gra and Res (Fig. 8a). Conversely, WTE_{SEAS} and STE_{SEAS} appear to be negatively correlated with Ped, Tc, Con_{SEAS_up}, Run_{SEAS_up} and Rc_{SEAS}. This set of explanatory variables falls into the VIP category with an average score > 0.8 (Fig. 8c). Finally, for both WTE and STE, the PLSR model has good predictive capacity (Fig. 8b), with coefficients of determination greater than 0.95.

4. Discussion

4.1. Increased erosion and runoff in the 10-m riparian zone without grass cover

The 10-m uncovered riparian zone (URZ) with teak trees and sparse understorey and litter cover showed high cumulative Run and Sed outflows downstream (Fig. 5). Sed shows a non-linear cumulative evolution in two phases that can be interpreted as the erosion of free particles on the surface (i.e., Fa and Fg) that are easily mobilised in the first phase, followed in the second phase, after this stock has been exhausted, by less intense erosion of particles embedded into the soil surface and requiring more energy to be mobilised (Ribolzi et al., 2011). Unlike the other riparian zone types, URZ showed negative trapping efficiency for both runoff water and sediment (Figs. 6 and 7), meaning that URZ acted as a net emitter of runoff water and sediment. We therefore conclude that, in addition to uphill inflow, runoff and sediment were generated within the URZ riparian zone. This is consistent with microplot observations showing high Rc_{SEAS} and SL_{SEAS} in URZ (Fig. 4). These observations corroborate those made on teak plantations in northern Laos, whether at the same study site (Patin et al., 2018) or on another experimental catchment (Song et al., 2020): as in our study (Table A.3), these previous works have shown an agreement between high soil loss and high runoff coefficient, particularly when the soil surface had low litter and vegetation cover, as well as low infiltrability due to high crusting rates (Patin et al., 2018).

Surface crusting, a process described by several authors (see for example Valentin and Bresson (1997)), affects the hydrodynamic properties of the soil surface, reducing its infiltrability (Bu et al., 2014; Casenave and Valentin, 1992). This process is observed in a range of climates and environments, often under intensive farming conditions (Valentin and Rajot, 2018). Our study shows that it can also occur in cultivated riparian environments of mountainous areas in the humid tropics. One of the main causes of crusting is the exposure of the soil surface to the impact of raindrops, commonly referred to as the “splash” effect (Mügler et al., 2019). In addition to causing the formation of an impervious crust, the “splash” effect is also one of the main processes responsible for the mobilisation and the downstream transfer of solid soil particles (Luk, 1979). Because of its very low-density understorey and its low litter cover, URZ soil surface is little protected from rainfall/throughfall and is particularly exposed to this erosion process, which explains the formation of pedestal features, and the high SL and Rc values observed in this zone.

Moreover, the “splash effect” can be exacerbated by the tree canopy which, depending on the morphology and size of the leaves, may cause raindrops to coalesce, thereby increasing the size of the throughfall drops and their kinetic energy on impact (Lacombe et al., 2018). Because of their large leaves with a morphology that favours the concentration of raindrops, soils under teak trees are particularly prone to the “splash” effect, which is generally put forward as an explanation for the very high rates of erosion and runoff in plantations (Ribolzi et al., 2017).

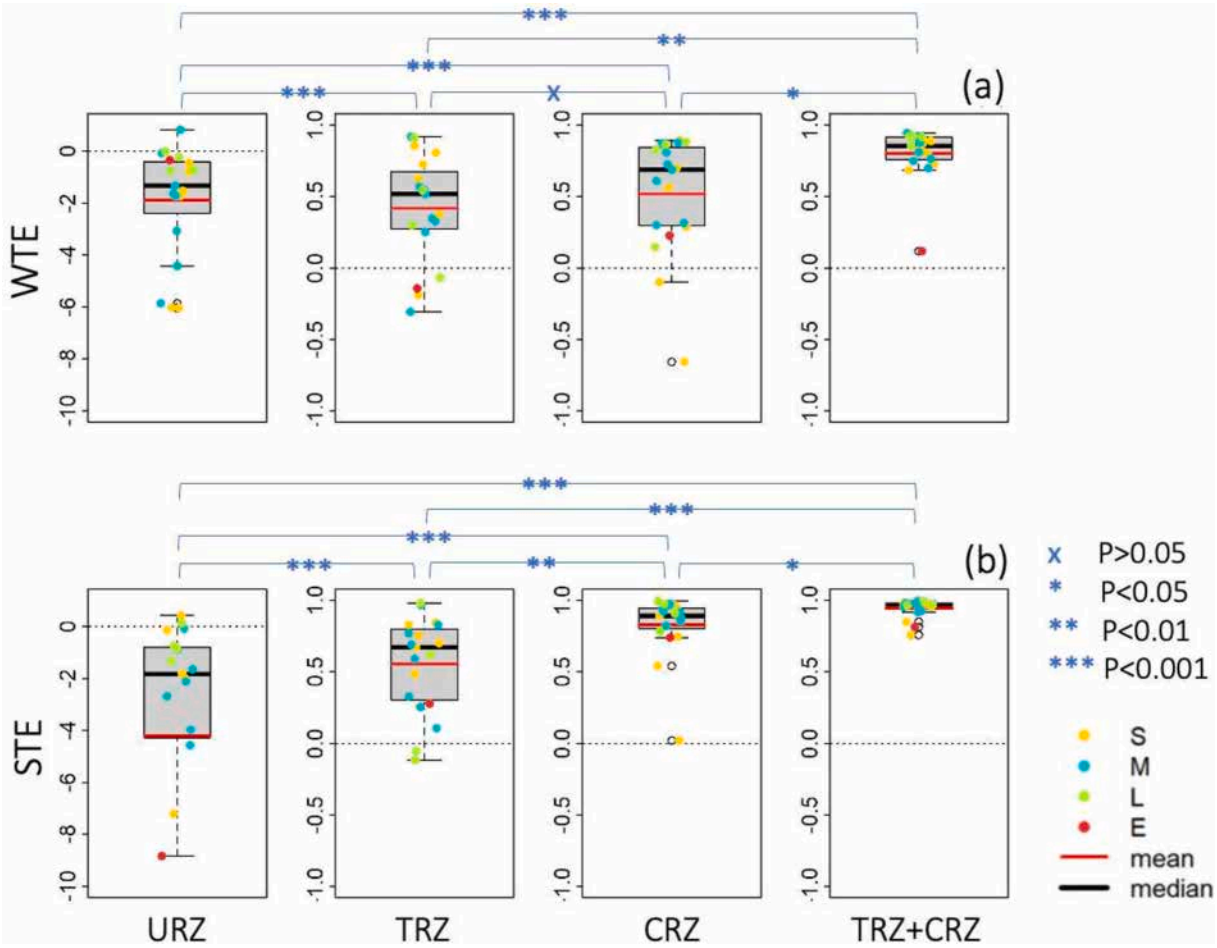

Fig. 7. Distributions of water and sediment trapping efficiency values measured in the different types of riparian zones. Boxplots of (a) water trapping efficiency (WTE) and (b) sediment trapping efficiency (STE) estimates using the 15 Gerlach trough installed in the four riparian zone types (i.e. URZ: 10 m wide uncovered riparian zone; TRZ: 5 m wide transitional riparian zone; CRZ: 5 m wide covered riparian zone; TRZ + CRZ: 10 m wide slope with TRZ uphill and CRZ downhill) and for the 19 rainfall events sampled between 6 July and 22 September 2014. For each boxplot, the horizontal black line is the median value, the horizontal red line is the average value, the upper and lower box hinges are the 25th and 75th percentiles, and the whiskers extend 1.5× the spread of the hinges. Data points outside the whiskers are outliers, indicated by white dots. WTE and STE values corresponding to small (S), medium (M), large (L) or exceptional (E) rainfall events (Table A.2) are indicated by yellow, blue, green and red dots respectively. The significance level of the Kruskal-Wallis test is indicated by horizontal lines linking compared pairs of boxplots: *** *p*-value<0.001; ** *p*-value <0.01; * *p*-value <0.05; x *p*-value >0.05 (non-significant). (For interpretation of the references to colour in this figure legend, the reader is referred to the web version of this article.)

4.2. Runoff water and sediment trapping in the 10-m riparian zone with grass cover

The 10-m-wide riparian zone with grass cover (TRZ + CRZ) had a cumulative outflow of water and sediment about 10 times lower than that of URZ (Fig. 6) and positive runoff water and sediment trapping efficiencies (Fig. 7). Such results can be interpreted as the consequence of two main phenomena:

- Firstly, due to the presence of a grass cover that reduces the kinetic energy of raindrops and hence protects the soil surface, TRZ + CRZ is not prone to the "splash" effect. As a result, TRZ + CRZ undergoes little soil loss compared to URZ (Fig. 4). Another consequence of grass cover protection against the "splash" effect is a lower rate of soil surface crusting (Table A.3) and therefore a greater infiltrability, explaining the lower runoff coefficients of TRZ + CRZ compared to that of URZ and, by way of consequence, the greater efficiency of TRZ + CRZ in trapping runoff water from the upstream teak plantation (Fig. 6). Mechanically, when the "splash" effect is limited, the reduced thickness of the runoff water due to infiltration decreases the hydraulic component of soil erosion (i.e. the "wash" effect) while favouring solid particles deposition (Mügler et al., 2019).
- Secondly, grass stems and fairly abundant litter on the soil surface of TRZ + CRZ (Fig. A.1) increase the tortuosity of the pathways available for runoff, thus reducing its average velocity. This result is in line with previous findings showing that leaf litter reduces runoff and sediment yield (Jourgholami et al., 2019; Jourgholami et al., 2022; Jourgholami and Labelle, 2020). As a result of surface flow deceleration and hydraulic roughness increase, infiltration is increased and the trapping of solid particles is enhanced (Borin et al., 2005; Deletic and Fletcher, 2006; Le Bissonnais et al., 2004). In addition, by reducing the velocity of runoff water, grass cover prevents the formation of concentrated flow paths such as rills at the soil surface, thereby improving water infiltration and the settling of suspended soil particles (Castelle et al., 1994).

In contrast to URZ, TRZ + CRZ had low Ped values, in line with a low erosion rate (Song et al., 2020), and high Wor values, indicating biological activity related to soil macrofauna, resulting in improved infiltration (Jouquet et al., 2008). As for URZ, areal percentages of pedestals (Ped) and worm casts (Wor) appear to be relevant indicators but, in the

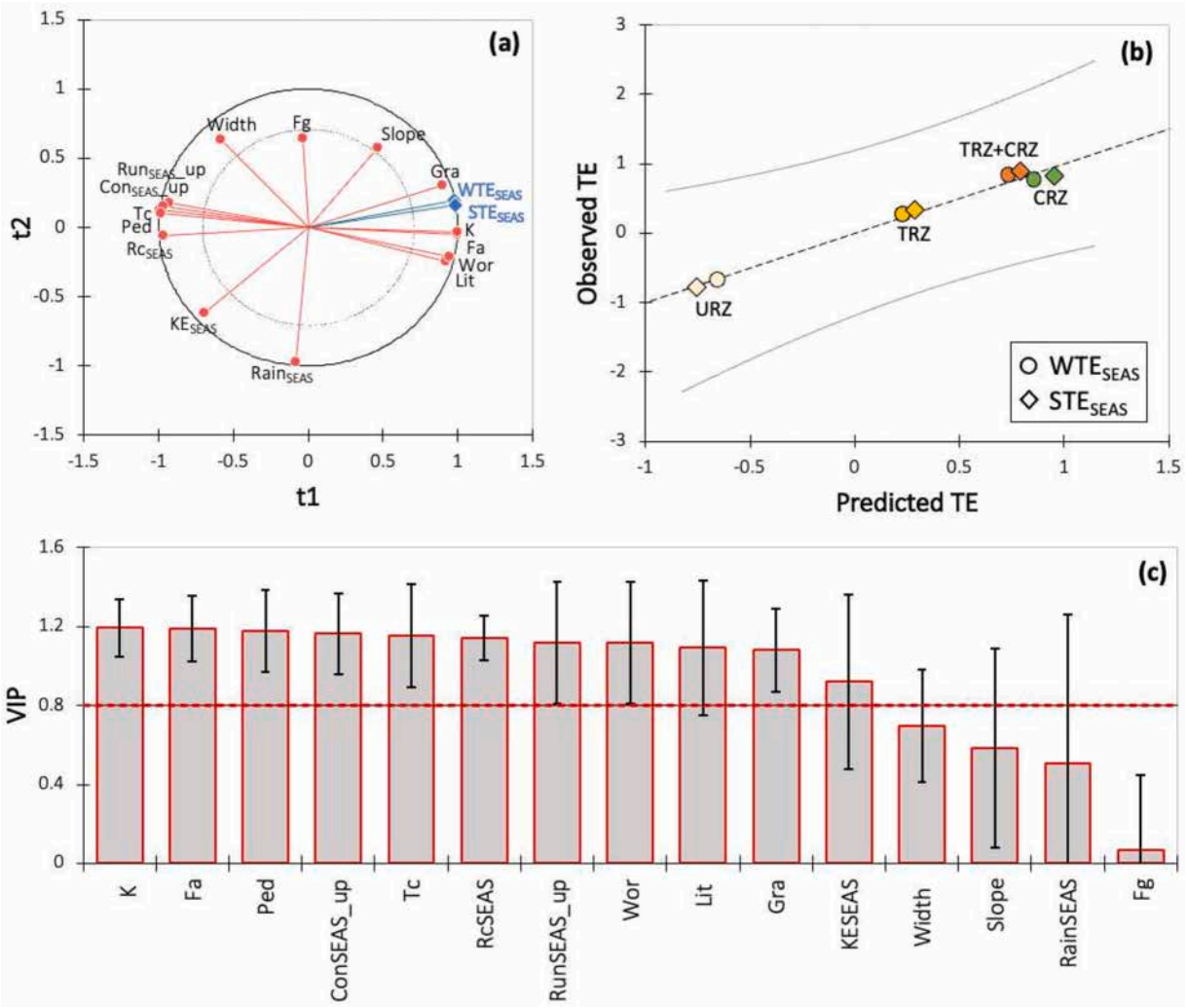

Fig. 8. Main results of the Partial Least Squares Regression (PLSR): (a) First plan of the analysis defined by the first two components (t1 and t2) and showing the position in relation to the circle of correlations of the two dependent variables (WTE_{SEAS} and STE_{SEAS}) and the 15 explanatory variables ($Rain_{SEAS}$, KE_{SEAS}, Fa, Fg, Tc, Lit, Wor, Ped, Gra, Slope, Width, K, Rc_{SEAS}, Run_{SEAS_up} and Con_{SEAS_up}); (b) Biplot showing the values of trapping efficiency (TE) for water (WTE_{SEAS}) and sediment (STE_{SEAS}) predicted by the PLSR model, and observed in the four types of riparian zones (CRZ, TRZ, TRZ + CRZ, URZ). The black dotted line represents the first bisector, and the light grey lines indicate the 95 % confidence interval. (c) Plot of Variable Importance in the Projection scores (VIP) and their coefficient of variation (CV) for the two components and the two models (WTE_{SEAS} and STE_{SEAS}). The horizontal red dotted line corresponds to the empirical value of 0.8 defined by Wold (1995) for the variables that contribute strongly to the models, and error black line corresponds to the standard deviation. (For interpretation of the references to colour in this figure legend, the reader is referred to the web version of this article.)

case of TRZ + CRZ, their high values correspond to an environment that is not conducive to soil detachment and surface runoff, resulting in positive STE and WTE.

4.3. *Trapping efficiency still significant with a 5-m riparian zone with grass cover*

The width of a grass buffer is generally considered to be a determining factor of its trapping efficiency. Grass buffer reported in the literature range in width from less than 5 to more than 200 m (Castelle et al., 1994) and have been tested in a wide variety of environments, using methods including field measurements under natural or simulated runoff conditions (Lou et al., 2022) and numerical modelling (Ziegler et al., 2006). For example, with a grassed buffer width of 6 m and a slope gradient of around 9 %, Miller et al. (2015) found STE values between 61 and 92 %. More recently, for the same buffer width, Luo et al. (2020) obtained values ranging between 77 and 81 % for the same slope gradient, and values between 59 and 72 % with a gradient of 36 %. With buffer widths equivalent to those tested in our study (i.e. 5- and 10-m), Abu-Zreig et al. (2004) showed that, for a slope gradient range of 2 to 5 %, the STE of 5- and 10-m wide grass buffers was 76–87 % and 86–97 %, respectively.

In our study, although average slope gradients were much higher (45–66 %), STE values were fairly comparable (Fig. 7) with interquartile ranges of 80–94 and 94–98 % for 5-m (CRZ) and 10-m (TRZ + CRZ) wide buffers, respectively. The interquartile range of STE was wider in the 5-m transitional zone (TRZ), at 30–80 %, with some low values close to zero (Fig. 7). The behaviour difference between TRZ and CRZ is probably related to the proportion of grass cover, which was only 18.5 % in TRZ. This hypothesis is consistent with the observations of Abu-Zreig et al. (2004), who showed an increasing logarithmic relationship between TSE and the percentage of vegetation cover.

4.4. *Factors controlling trapping efficiency, advantages and limitations of the PLSR analysis*

The PLSR model shows strong predictive power, particularly due to the large number of explanatory variables considered in the analysis (i.e.

15). However, although the model performs well in the context of the Houay Pano catchment (Fig. 1), it is important to bear in mind that it cannot be used on sites in other geographical contexts, given that it is based on a small number of observation sites (i.e. 4). Its main interest in the context of this study is to provide a summary of the main results, and in particular to highlight and rank the key explanatory variables for WTE_{SEAS} and STE_{SEAS}.

As previously stated, it appears that saturated hydraulic conductivity of the soil surface and areal percentages of litter and grass cover are factors that improve the trapping of runoff water and suspended sediment. This is in good agreement with the literature (Abu-Zreig et al., 2004; Castelle et al., 1994). The PLSR analysis also confirms that Ped and Wor are relevant indicators of the hydro-sedimentary functioning of the soil surface in the riparian zone: the presence of Wor indicates a better ability for trapping water and sediment, while Ped, on the contrary, reveals poor conditions or even a context likely to produce runoff and sediment. Similarly, in agreement with the literature (Luo et al., 2020; Patin et al., 2018; Vigiak et al., 2008), sediment concentration (Con), crusting rate (Tc), runoff coefficient (Rc) have an unfavourable effect on the trapping of water and sediment from surface runoff.

Of these 15 explanatory variables, slope gradient had a VIP score of less than 0.8 (Fig. 8). However, according to observations reported in the literature, the slope gradient is thought to have a major effect on STE, with low trapping efficiency when slope increases (Mekonnen et al., 2014; Jourgholami et al., 2021). The lack of influence of the slope gradient in our study can probably be explained by the range of values explored. Most previous studies have been carried out with slopes that rarely exceed 35 % (Luo et al., 2020) which is much less than slopes on which farmers grow rainfed crops in many mountainous agro-ecosystems of the humid tropics; in Southeast Asia for example, slope gradients without terraces often exceed 75 % (Ribolzi et al., 2011). In our study, such extreme conditions were better considered, with average slope gradients ranging from 45 to 66 % in the four studied riparian buffer zones. Despite such steep environments, WTE and STE of the 10-m wide grass remained positive and, if we disregard the exceptional rainfall of 17 September 2014, within ranges of 68–95 % and 76–99 %, respectively (Fig. 7).

4.5. Methodological approach and long-term benefits of grassed buffers

This study was designed as an endeavour to acquire scientifically sound observations and data that can be used as a basis for discussion and negotiation with stakeholders (i.e. farmers, local authorities, political decision-makers, etc.) to encourage the deployment and adoption of riparian vegetation buffer buffers as a nature-based solution to mitigate soil erosion. This overarching orientation led us to opt for investigations carried out under field conditions with natural rainfall rather than under controlled experimental conditions (Lou et al., 2022), or resorting to numerical modelling (Ziegler et al., 2006). Due to the variable intensity of natural rainfall during single events, this approach has the disadvantage of not allowing estimates based on measurements under steady-state flow conditions. In addition, characterization of hydrodynamics properties had to be carried out using replicate microplots, which are known to inappropriately capture processes that control runoff at larger scales (such preferential flow pathways or patterns of vegetation and soil surface conditions) (Sidle et al., 2007). However, despite the difficulties of carrying out this type of experiment in a remote mountainous environment with limited access, we were able to estimate WTE and STE for almost all the surface runoff events over the course of a full rainy season (19 out of 20), and to make observations during a wide range of rainfall event types (Table A.4).

To estimate WTE and STE, and in order to minimise the impact of the measurement device on surface runoff, we opted for the use of Gerlach troughs, which, unlike experimental plots delimited by a physical boundary (i.e. a metal frame), do not pose problems of edge effects, although they require multiple measurement points upstream and downstream of the area under investigation (Comino et al., 2016). This system proved effective for sampling all the rainfall-runoff events, with the exception of the exceptional event of 17 September, during which the volumetric capacity of the buckets was exceeded and the troughs filled with coarse sediment in URZ (Fig. 2f).

The results of this study reveal the short-term (i.e. time scales ranging from a single runoff event to the rainy season) effectiveness of grassed buffers in trapping surface runoff water and sediment. However, in the medium to long term (decennial or more), the trapping efficiency of vegetated riparian buffer zones and the balance of sediment exports to the stream is questionable. Indeed, it is likely that sediment accumulation in a narrow buffer will eventually modify the morphological profile of the hillslope adjacent to the stream (Chaplot et al., 2005). The gradual increase in the mass of soil deposits in an area with a steep slope gradient, combined with the lateral circulation of subsurface water on the hillslope (Ziegler et al., 2006) due to the good permeability of the grassed soil, are all factors that increase the risk of shallow landslides towards the stream. Associating trees with the herbaceous cover in the riparian zone, so that the soil can be maintained and strengthened by the roots of the woody plants, either directly (Marzini et al., 2023) or from drawdown of soil moisture (Kim et al., 2017) may limit this risk.

5. Conclusion

We assessed the effect of riparian grass buffers on surface runoff, soil loss, sediment exports, and water and sediment trapping efficiencies in teak plantations in the uplands of northern Lao PDR. We showed that conserving <10 m riparian grass buffers on steep hillslopes planted with teak trees was sufficient to reduce soil loss by a factor of 23, with water and sediment trapping efficiencies of 82 % and 89 %, respectively, although trapping was less effective during exceptional rainfall events (24-h rainfall >84.5 mm). This work also found that the best predictors of soil loss were saturated soil hydraulic conductivity, areal percentages of grass and litter, soil crusting, and free aggregates. Based on the experimental evidence gained through this study, we therefore recommend that riparian grass buffers 10 m wide are maintained in teak plantations in the uplands of northern Lao PDR.

Compared to previous work in the same context (Song et al., 2020), this study further indicates that maintaining riparian grass buffers of at least 10 m is an effective way of mitigating soil loss on hillslopes and ensuring the sustainability of agricultural productivity. The present study also showed that riparian grass buffers can be more effective at trapping sediment-laden runoff when combined with understorey conservation practices. By reducing surface runoff and soil loss, riparian grass buffers can also be expected to reduce the risk of stream pollution, particularly from chemical and bacteriological contaminants attached to suspended sediments (Boithias et al., 2024). From the results of this and previous work (Song et al., 2020), we recommend limiting soil erosion on the upstream slope as much as possible, i.e., by maintaining high-density understorey in plantations, whether natural or planted with a cash crop such as broom grass.

Involving stakeholders, including farmers in the design and implementation of research may increase their awareness of soil conservation and improve the adoption of conservation practices (Cooper et al., 1996; Shelton et al., 2009).

Further research is needed to assess whether riparian grass can be used to mitigate surface runoff and soil loss at the scale of entire catchment areas.

Funding

This work was supported by the French National Research Agency (TecItEasy and DinBuam projects, ANR-13-AGRO-0007 and ANR-22-CE3-0006 respectively). Layheang Song received a scholarship from the Ministry of Education, Youth and Sports of Cambodia (928762L) and the French government (928719A) to carry out this work. This study was

supported by the French Research Institute for sustainable development (IRD) through the international joint laboratory LUSES (Dynamic of Land Use Changes and Soil Ecosystem Services).

CRediT authorship contribution statement

Layheang Song: Writing – original draft, Validation, Formal analysis, Data curation. **Olivier Ribolzi:** Writing – review & editing, Supervision, Methodology, Investigation, Funding acquisition, Conceptualization. **Laurie Boithias:** Writing – review & editing, Supervision, Methodology. **Khampaseuth Xayyathip:** Investigation. **Christian Valentin:** Investigation, Data curation. **Bounsamay Soulileuth:** Investigation. **Henri Robain:** Investigation. **Anneke de Rouw:** Investigation. **Phabvilay Sounyafong:** Investigation. **Norbert Silvera:** Investigation. **Phimmasone Sisouvanh:** Supervision. **Jean-Louis Janeau:** Investigation. **Inpeng Saveng:** Investigation. **Chantha Oeurng:** Supervision. **Alain Pierret:** Writing – review & editing, Investigation.

Declaration of competing interest

The authors declare that they have no known competing financial interests or personal relationships that could have appeared to influence the work reported in this paper.

Data availability

https://doi.org/10.23708/4GTSHN

Acknowledgments

The sampling and laboratory experiment were performed with the help of two students of the Faculty of Agriculture (National University of Laos), namely Siviengkhone DIMAK and Jinthala KEOMANYSONE. The authors sincerely thank the M-TROPICS Critical Zone Observatory (https://mtropics.obs-mip.fr/), which belongs to the French Research Infrastructure OZCAR (http://www.ozcar-ri.org/), for long-term data access, and the Lao Department of Agricultural Land Management (DALaM) for its support, including granting the permission for field access.

Appendix A. Supplementary data

Supplementary data to this article can be found online at https://doi.org/10.1016/j.ecoleng.2025.107537.

References

Abdi, H., 2010. Partial least squares regression and projection on latent structure regression (PLS Regression). Wiley Interdisciplinary Rev. Computat. Stat. 2 (1), 97–106. https://doi.org/10.1002/wics.51.

Abu-Zreig, M., Rudra, R.P., Lalonde, M.N., Whiteley, H.R., Kaushik, N.K., 2004. Experimental investigation of runoff reduction and sediment removal by vegetated filter strips. Hydrol. Process. 18 (11), 2029–2037. https://doi.org/10.1002/hyp.1400.

Addinsoft, 2021. XLSTAT Statistical and Data Analysis Solution. New York, USA. Retrieved from. https://www.xlstat.com.

Ahmad, N.S.B.N., Mustafa, F.B., Gideon, D., 2020. A systematic review of soil erosion control practices on the agricultural land in Asia. Int. Soil Water Conservat. Res. 8 (2), 103–115. https://doi.org/10.1016/j.iswcr.2020.04.001.

Alemu, T., Bahrndorff, S., Hundera, K., Alemayehu, E., Ambelu, A., 2017. Effect of riparian land use on environmental conditions and riparian vegetation in the east African highland streams. Limnologica 66, 1–11. https://doi.org/10.1016/j.limno.2017.07.001.

Angelsen, A., & Kaimowitz, D. (2004). Is agroforestry likely to reduce deforestation. In G. Schroth, G. A. d. Fonseca, C. A. Harvey, C. Gascon, H. L. Vasconcelos, & A.-M. N. Izac (Eds.), Agroforestry and Biodiversity Conservation in Tropical Landscapes (pp. 87–106). Washington, DC: Island Press.

Bereswill, R., Streloke, M., Schulz, R., 2014. Risk mitigation measures for diffuse pesticide entry into aquatic ecosystems: proposal of a guide to identify appropriate measures on a catchment scale. Integr. Environ. Assess. Manag. 10 (2), 286–298. https://doi.org/10.1002/ieam.1517.

Bhat, S.A., Dar, M.U.D., Meena, R.S., 2019. Soil erosion and management strategies. In: Sustainable Management of Soil and Environment. Springer, pp. 73–122. https://doi.org/10.1007/978-981-13-8832-3_3.

Boithias, L., Auda, Y., Audry, S., Bricquet, J.-P., Chanhphengxay, A., Chaplot, V., Xayyathip, K., 2021a. The Multiscale TROPIcal CatchmentS critical zone observatory M-TROPICS dataset II: land use, hydrology and sediment production monitoring in Houay Pano, northern Lao PDR. Hydrol. Process. 35 (5), e14126. https://doi.org/10.1002/hyp.14126.

Boithias, L., Ribolzi, O., Lacombe, G., Thammahacksa, C., Silvera, N., Latsachack, K., Rochelle-Newall, E., 2021b. Quantifying the effect of overland flow on Escherichia coli pulses during floods: use of a tracer-based approach in an erosion-prone tropical catchment. J. Hydrol. 594, 125935. https://doi.org/10.1016/j.jhydrol.2020.125935.

Boithias, L., Jardé, E., Latsachack, K., Thammahacksa, C., Silvera, N., Soulileuth, B., Ribolzi, O., 2024. Village Settlements in Mountainous Tropical areas, Hotspots of Fecal Contamination as Evidenced by Escherichia coli and Stanol Concentrations in Stormwater Pulses. Environ. Sci. Technol. 58, 6335–6348. https://doi.org/10.1021/acs.est.3c09090.

Borin, M., Vianello, M., Morari, F., Zanin, G., 2005. Effectiveness of buffer strips in removing pollutants in runoff from a cultivated field in North-East Italy. Agric. Ecosyst. Environ. 105 (1–2), 101–114. https://doi.org/10.1016/j.agee.2004.05.011.

Borrelli, P., Robinson, D.A., Fleischer, L.R., Lugato, E., Ballabio, C., Alewell, C., Panagos, P., 2017. An assessment of the global impact of 21st century land use change on soil erosion. Nat. Commun. 8 (1), 2013. https://doi.org/10.1038/s41467-017-02142-7.

Bu, C.-F., Wu, S.-F., Yang, K.-B., 2014. Effects of physical soil crusts on infiltration and splash erosion in three typical Chinese soils. Int. J. Sedim. Res. 29 (4), 491–501. https://doi.org/10.1016/S1001-6279(14)60062-7.

Calder, I.R., 2001. Canopy processes: Implications for transpiration, interception and splash induced erosion, ultimately for forest management and water resources. In: Linsenmair, K.E., Davis, A.J., Fiala, B., Speight, M.R. (Eds.), Tropical Forest Canopies: Ecology and Management: Proceedings of ESF Conference, Oxford University, 12–16 December 1998. Springer Netherlands, Dordrecht, pp. 203–214. https://doi.org/10.1007/978-94-017-3606-0_16.

Calder, I.R., Amezaga, J.M., Aylward, B., Bosch, J., Fuller, L., Gallop, K., Miranda, M., 2004. Forest and Water policies. The need to reconcile public and science perceptions. Geol. Acta 2 (2), 157–166. https://doi.org/10.1344/105.000001436.

Cao, X., Song, C., Xiao, J., Zhou, Y., 2018. The optimal width and mechanism of riparian buffers for storm water nutrient removal in the Chinese eutrophic Lake Chaohu watershed. Water 10 (10), 1489. https://doi.org/10.3390/w10101489.

Casenave, A., Valentin, C., 1992. A runoff capability classification system based on surface features criteria in semi-arid areas of West Africa. J. Hydrol. 130 (1–4), 231–249. https://doi.org/10.1016/0022-1694(92)90112-9.

Castelle, A.J., Johnson, A., Conolly, C., 1994. Wetland and stream buffer size requirements—a review. J. Environ. Qual. 23 (5), 878–882. https://doi.org/10.2134/jeq1994.00472425002300050004x.

Chaplot, V., Le Brozec, E.C., Silvera, N., Valentin, C., 2005. Spatial and temporal assessment of linear erosion in catchments under sloping lands of northern Laos. Catena 63 (2–3), 167–184. https://doi.org/10.1016/j.catena.2005.06.003.

Comino, J.R., Quiquerez, A., Follain, S., Raclot, D., Le Bissonnais, Y., Casalí, J., Brevik, E., 2016. Soil erosion in sloping vineyards assessed by using botanical indicators and sediment collectors in the Ruwer-Mosel valley. Agric. Ecosyst. Environ. 233, 158–170. https://doi.org/10.1016/j.agee.2016.09.009.

Cooper, P.J.M., Leakey, R.R.B., Rao, M.R., Reynolds, L., 1996. Agroforestry and the Mitigation of Land Degradation in the Humid and Sub-humid Tropics of Africa. Exp. Agric. 32 (3), 235–290. https://doi.org/10.1017/S0014479700026223.

de Rouw, A., Ribolzi, O., Douillet, M., Tjantahosong, H., Soulileuth, B., 2018. Weed seed dispersal via runoff water and eroded soil. Agric. Ecosyst. Environ. 265, 488–502. https://doi.org/10.1016/j.agee.2018.05.026.

Deletic, A., Fletcher, T.D., 2006. Performance of grass filters used for stormwater treatment—a field and modelling study. J. Hydrol. 317 (3–4), 261–275. https://doi.org/10.1016/j.jhydrol.2005.05.021.

Ding, W., He, X., Chen, W., 2011. Runoff and sediment reduction by riparian buffer filters on steep slopes. In: Paper presented at the 2011 International Conference on Computer distributed Control and Intelligent Environmental monitoring, pp. 998–1001. https://doi.org/10.1109/CDCIEM.2011.147.

Dong, Y., Xiong, D., Su, Z., a., Yang, D., Zheng, X., Shi, L., & Poesen, J., 2018. Effects of vegetation buffer strips on concentrated flow hydraulics and gully bed erosion based on in situ scouring experiments. Land Degrad. Dev. 29 (6), 1672–1682. https://doi.org/10.1002/ldr.2943.

Dosskey, M.G., Vidon, P., Gurwick, N.P., Allan, C.J., Duval, T.P., Lowrance, R., 2010. The role of riparian vegetation in protecting and improving chemical water quality in streams 1. J. Am. Water Resour. Assoc. 46 (2), 261–277. https://doi.org/10.1111/j.1752-1688.2010.00419.x.

Dregne, H.E., 1995. Erosion and soil productivity in Australia and New Zealand. Land Degrad. Dev. 6 (2), 71–78. https://doi.org/10.1002/ldr.3400060202.

Foltz, R.B., Copeland, N.S., Elliot, W.J., 2009. Reopening abandoned forest roads in northern Idaho, USA: Quantification of runoff, sediment concentration, infiltration, and interrill erosion parameters. J. Environ. Manag. 90 (8), 2542–2550. https://doi.org/10.1016/j.jenvman.2009.01.014.

Gerlach, T., 1967. Hillslope troughs for measuring sediment movement. Rev. Géomorphol. Dynam. 17, 173.

Gumiere, S.J., Le Bissonnais, Y., Raclot, D., Cheviron, B., 2011. Vegetated filter effects on sedimentological connectivity of agricultural catchments in erosion modelling: a review. Earth Surf. Process. Landf. 36 (1), 3–19. https://doi.org/10.1002/esp.2042.

Huon, S., Evrard, O., Gourdin, E., Lefèvre, I., Bariac, T., Reyss, J.-L., Ribolzi, O., 2017. Suspended sediment source and propagation during monsoon events across nested sub-catchments with contrasted land uses in Laos. J. Hydrol. 9, 69–84. https://doi.org/10.1016/j.ejrh.2016.11.018.

Jouquet, P., Podwojewski, P., Bottinelli, N., Mathieu, J., Ricoy, M., Orange, D., Valentin, C., 2008. Above-ground earthworm casts affect water runoff and soil erosion in Northern Vietnam. Catena 74 (1), 13–21. https://doi.org/10.1016/j.catena.2007.12.006.

Jourgholami, M., Labelle, E.R., 2020. Effects of plot length and soil texture on runoff and sediment yield occurring on machine-trafficked soils in a mixed deciduous forest. Ann. For. Sci. 77, 19. https://doi.org/10.1007/s13595-020-00938-0.

Jourgholami, M., Labelle, E.R., Feghhi, J., 2019. Efficacy of leaf litter mulch to mitigate runoff and sediment yield following mechanized operations in the Hyrcanian mixed forests. J. Soils Sediments 19, 2076–2088. https://doi.org/10.1007/s11368-018-2194-x.

Jourgholami, M., Karami, S., Tavankar, F., Lo Monaco, A., Picchio, R., 2021. Effects of slope gradient on runoff and sediment yield on machine-induced compacted soil in temperate forests. Forests 12 (1), 49. https://doi.org/10.3390/f12010049.

Jourgholami, M., Sohrabi, H., Venanzi, R., Tavankar, F., Picchio, R., 2022. Hydrologic responses of undecomposed litter mulch on compacted soil: Litter water holding capacity, runoff, and sediment. Catena 210, 105875. https://doi.org/10.1016/j.catena.2021.105875.

Kagabo, D., Stroosnijder, L., Visser, S., Moore, D., 2013. Soil erosion, soil fertility and crop yield on slow-forming terraces in the highlands of Buberuka, Rwanda. Soil Tillage Res. 128, 23–29. https://doi.org/10.1016/j.still.2012.11.002.

Kim, J.H., Fourcaud, T., Jourdan, C., Maeght, J.-L., Mao, Z., Metayer, J., Stokes, A., 2017. Vegetation as a driver of temporal variations in slope stability: the impact of hydrological processes. Geophys. Res. Lett. 44 (10), 4897–4907. https://doi.org/10.1002/2017GL073174.

Kinnell, P., 1981. Rainfall Intensity-Kinetic Energy Relationships for Soil loss Prediction. Soil Sci. Soc. Am. J. 45 (1), 153–155. https://doi.org/10.2136/sssaj1981.03615995004500010033x.

Lacombe, G., Ribolzi, O., de Rouw, A., Pierret, A., Latsachak, K., Silvera, N., Valentin, C., 2016. Contradictory hydrological impacts of afforestation in the humid tropics evidenced by long-term field monitoring and simulation modelling. Hydrol. Earth Syst. Sci. 20 (7), 2691–2704. https://doi.org/10.5194/hess-20-2691-2016.

Lacombe, G., Valentin, C., Sounyafong, P., de Rouw, A., Soulileuth, B., Silvera, N., Ribolzi, O., 2018. Linking crop structure, throughfall, soil surface conditions, runoff and soil detachment: 10 land uses analyzed in Northern Laos. Sci. Total Environ. 616-617, 1330–1338. https://doi.org/10.1016/j.scitotenv.2017.10.185.

Le Bissonnais, Y., Lecomte, V., Cerdan, O., 2004. Grass strip effects on runoff and soil loss. Agronomie 24 (3), 129–136. https://doi.org/10.1051/agro:2004010.

Le, H.T., Rochelle-Newall, E., Ribolzi, O., Janeau, J.L., Huon, S., Latsachack, K., Pommier, T., 2020. Land use strongly influences soil organic carbon and bacterial community export in runoff in tropical uplands. Land Degrad. Dev. 31 (1), 118–132. https://doi.org/10.1002/ldr.3433.

Lestrelin, G., Giordano, M., 2007. Upland development policy, livelihood change and land degradation: interactions from a Laotian village. Land Degrad. Dev. 18 (1), 55–76. https://doi.org/10.1002/ldr.756.

Lou, Y., Gao, Z., Li, Y., Sun, G., Wu, T., Cen, Y., Su, B., 2022. Effects of Distributions of Grass strips on Soil Erosion in Spoil Tips. Water 14 (6), 913. https://doi.org/10.3390/w14060913.

Luk, S.H., 1979. Effect of soil properties on erosion by wash and splash. Earth Surface Proces. 4 (3), 241–255. https://doi.org/10.1002/esp.3290040305.

Luke, S.H., Slade, E.M., Gray, C.L., et al., 2019. Riparian buffers in tropical agriculture: Scientific support, effectiveness and directions for policy. J. Appl. Ecol. 56, 85–92. https://doi.org/10.1111/1365-2664.13280.

Luo, M., Pan, C., Liu, C., 2020. Experiments on measuring and verifying sediment trapping capacity of grass strips. Catena 194, 104714. https://doi.org/10.1016/j.catena.2020.104714.

Marzini, L., D'Addario, E., Papasidero, M.P., Chianucci, F., Disperati, L., 2023. Influence of root Reinforcement on Shallow Landslide distribution: A Case Study in Garfagnana (Northern Tuscany, Italy). Geosciences 13 (11), 326. https://doi.org/10.3390/geosciences13110326.

McKergow, L.A., Prosser, I.P., Grayson, R.B., Heiner, D., 2004a. Performance of grass and rainforest riparian buffers in the wet tropics, Far North Queensland. 2. Water quality. Soil Res. 42 (4), 485–498. https://doi.org/10.1071/SR02156.

McKergow, L.A., Prosser, I.P., Grayson, R.B., Heiner, D., 2004b. Performance of grass and rainforest riparian buffers in the wet tropics, Far North Queensland. 1. Riparian hydrology. Aust. J. Soil Res. 41 (4). https://doi.org/10.1071/SR02155.

Mekonnen, M., Keesstra, S.D., Stroosnijder, L., Baartman, J.E., Maroulis, J., 2014. Soil conservation through sediment trapping: a review. Land Degrad. Dev. 26 (6), 544–556. https://doi.org/10.1002/ldr.2308.

Miller, J.J., Curtis, T., Chanasyk, D.S., Reedyk, S., 2015. Influence of mowing and narrow grass buffer widths on reductions in sediment, nutrients, and bacteria in surface runoff. Can. J. Soil Sci. 95 (2), 139–151. https://doi.org/10.4141/cjss-2014-082.

Miyata, S., Kosugi, K., i., Gomi, T., & Mizuyama, T., 2009. Effects of forest floor coverage on overland flow and soil erosion on hillslopes in Japanese cypress plantation forests. Water Resour. Res. 45 (6). https://doi.org/10.1029/2008WR007270.

Mügler, C., Ribolzi, O., Janeau, J.-L., Rochelle-Newall, E., Latsachack, K., Thammahacksa, C., Valentin, C., 2019. Experimental and modelling evidence of short-term effect of raindrop impact on hydraulic conductivity and overland flow intensity. J. Hydrol. 570, 401–410. https://doi.org/10.1016/j.jhydrol.2018.12.046.

Neyret, M., Robain, H., de Rouw, A., Janeau, J.-L., Durand, T., Kaewthip, J., Valentin, C., 2020. Higher runoff and soil detachment in rubber tree plantations compared to annual cultivation is mitigated by ground cover in steep mountainous Thailand. Catena 189, 104472. https://doi.org/10.1016/j.catena.2020.104472.

Pan, D., Gao, X., Wang, J., Yang, M., Wu, P., Huang, J., Zhao, X., 2018. Vegetative filter strips—effect of vegetation type and shape of strip on run-off and sediment trapping. Land Degrad. Dev. 29 (11), 3917–3927. https://doi.org/10.1002/ldr.3160.

Patin, J., Mouche, E., Ribolzi, O., Sengtahevanghoung, O., Latsachak, K.O., Soulileuth, B., Valentin, C., 2018. Effect of land use on interrill erosion in a montane catchment of Northern Laos: an analysis based on a pluri-annual runoff and soil loss database. J. Hydrol. 563, 480–494. https://doi.org/10.1016/j.jhydrol.2018.05.044.

Perron, T., Legrand, M., Janeau, J.-L., Manizan, A., Vierling, C., Kouakou, A., Mareschal, L., 2024. Runoff and soil loss are drastically decreased in a rubber plantation combining the spreading of logging residues with a legume cover. Sci. Total Environ. 913, 169335. https://doi.org/10.1016/j.scitotenv.2023.169335.

Pimentel, D., 2006. Soil erosion: a food and environmental threat. Environ. Dev. Sustain. 8 (1), 119–137. https://doi.org/10.1007/s10668-005-1262-8.

Ribolzi, O., Patin, J., Bresson, L.M., Latsachack, K.O., Mouche, E., Sengtaheuanghoung, O., Valentin, C., 2011. Impact of slope gradient on soil surface features and infiltration on steep slopes in northern Laos. Geomorphology 127 (1–2), 53–63. https://doi.org/10.1016/j.geomorph.2010.12.004.

Ribolzi, O., Evrard, O., Huon, S., de Rouw, A., Silvera, N., Latsachack, K.O., Valentin, C., 2017. From shifting cultivation to teak plantation: effect on overland flow and sediment yield in a montane tropical catchment. Sci. Rep. 7 (1), 3987. https://doi.org/10.1038/s41598-017-04385-2.

Ribolzi, O., Xayyathip, K., Christian, V., Soulileuth, B., Robain, H., De Rouw, A., Sounyafong, P., Silvera, N., Janeau, J.-L., 2024. Rainfall, surface runoff, soil erosion, soil physical properties and soil surface features in teak tree plantations, Houay Pano catchment, Northern Lao PDR (2001-2019) [Data Set]. DataSuds. https://doi.org/10.23708/4GTSHN.

Sanz, M., De Vente, J., Chotte, J.-L., Bernoux, M., Kust, G., Ruiz, I., Castillo, V., 2017. Sustainable Land Management Contribution to Successful Land-Based Climate Change Adaptation and Mitigation. A Report of the Science-Policy Interface, United Nations Convention to Combat Desertification (UNCCD), Bonn, Germany.

Sartori, M., Philippidis, G., Ferrari, E., Borrelli, P., Lugato, E., Montanarella, L., Panagos, P., 2019. A linkage between the biophysical and the economic: Assessing the global market impacts of soil erosion. Land Use Policy 86, 299–312. https://doi.org/10.1016/j.landusepol.2019.05.014.

Sharma, N., Singh, R.J., Mandal, D., Kumar, A., Alam, N., Keesstra, S., 2017. Increasing farmer's income and reducing soil erosion using intercropping in rainfed maize-wheat rotation of Himalaya, India. Agric. Ecosyst. Environ. 247, 43–53. https://doi.org/10.1016/j.agee.2017.06.026.

Shelton, D.P., Wilke, R.A., Franti, T.G., Josiah, S.J., 2009. Farmlink: promoting conservation buffers farmer-to-farmer. Agrofor. Syst. 75 (1), 83–89. https://doi.org/10.1007/s10457-008-9130-9.

Sidle, R.C., Ziegler, A.D., Negishi, J.N., Nik, A.R., Siew, R., Turkelboom, F., 2006. Erosion processes in steep terrain—truths, myths, and uncertainties related to forest management in Southeast Asia. For. Ecol. Manag. 224 (1–2), 199–225. https://doi.org/10.1016/j.foreco.2005.12.019.

Sidle, R.C., Hirano, T., Gomi, T., Terajima, T., 2007. Hortonian overland flow from Japanese forest plantations; an aberration, the real thing, or something in between? Hydrol. Process. 21 (23), 3237–3247. https://doi.org/10.1002/hyp.6876.

Song, L., Boithias, L., Sengtaheuanghoung, O., Oeurng, C., Valentin, C., Souksavath, B., Ribolzi, O., 2020. Understory Limits Surface Runoff and Soil loss in Teak tree Plantations of Northern Lao PDR. Water 12 (9), 2327. https://doi.org/10.3390/w12092327.

Thomaz, E.L., 2009. The influence of traditional steep land agricultural practices on runoff and soil loss. Agric. Ecosyst. Environ. 130 (1–2), 23–30. https://doi.org/10.1016/j.agee.2008.11.009.

Valentin, C., Bresson, L.M., 1997. Soil Crusting. In: Lal, R., Blum, W.E.H., Valentin, C., Stewart, B.A. (Eds.), Methods for Assessment of Soil Degradation, 1st ed. CRC Press, Boca Raton, p. 576. https://doi.org/10.1201/9781003068716.

Valentin, C., Rajot, J.L., 2018. Erosion and Principles of Soil Conservation. In: Soils as a Key Component of the critical Zone 5: Degradation and Rehabilitation, 5, pp. 39–82. https://doi.org/10.1002/9781119438298.ch3.

Van Dijk, A., Bruijnzeel, L., Rosewell, C., 2002. Rainfall intensity–kinetic energy relationships: a critical literature appraisal. J. Hydrol. 261 (1–4), 1–23. https://doi.org/10.1016/S0022-1694(02)00020-3.

van Meerveld, H., Jones, J.P., Ghimire, C.P., Zwartendijk, B.W., Lahitiana, J., Ravelona, M., Mulligan, M., 2021. Forest regeneration can positively contribute to local hydrological ecosystem services: Implications for forest landscape restoration. J. Appl. Ecol. 58 (4), 755–765. https://doi.org/10.1111/1365-2664.13836.

Vidon, P.G., Hill, A.R., 2004. Landscape controls on nitrate removal in stream riparian zones. Water Resour. Res. 40 (3). https://doi.org/10.1029/2003WR002473.

Vigiak, O., Ribolzi, O., Pierret, A., Sengtaheuanghoung, O., Valentin, C., 2008. Trapping efficiencies of cultivated and natural riparian vegetation of northern Laos. J. Environ. Qual. 37 (3), 889–897. https://doi.org/10.2134/jeq2007.0251.

Wei, X., Sauvage, S., Le, T.P.Q., Ouillon, S., Orange, D., Vinh, V.D., Sanchez-Perez, J.-M., 2019. A Modeling Approach to Diagnose the Impacts of Global changes on Discharge and Suspended Sediment Concentration within the Red River Basin. Water 11 (5), 958. https://doi.org/10.3390/w11050958.

Wiersum, K., 1985. Effects of various vegetation layers in an Acacia auriculiformis forest plantation on surface erosion in Java, Indonesia.

Wold, S. (1995). PLS for multivariate linear modeling. In H. v. d. Waterbeemd (Ed.), Chemometric Methods in Molecular Design (Vol. vol. 17, pp. 195–218). Weinheim, Germany: Wiley-VCH. doi:https://doi.org/10.1002/9783527615452.

Wuepper, D., Borrelli, P., Finger, R., 2020. Countries and the global rate of soil erosion. Nat. Sustainabil. 3 (1), 51–55. https://doi.org/10.1038/s41893-019-0438-4.

Xaysatith, S., Alain, P., Vidhaya, T.-g., Supat Isarangkool Na, A., Saysongkham, S., & Christian, H. (2022). Does forest conversion to tree plantations affect properties of subsoil horizons? Findings from mainland Southeast Asia (Lao PDR, Yunnan-China). Geoderma Reg., 28, e00457. doi:https://doi.org/10.1016/j.geodrs.2021.e00457.

Ziegler, A.D., Tran, L.T., Giambelluca, T.W., Sidle, R.C., Sutherland, R.A., Nullet, M.A., Vien, T.D., 2006. Effective slope lengths for buffering hillslope surface runoff in fragmented landscapes in northern Vietnam. For. Ecol. Manag. 224 (1–2), 104–118. https://doi.org/10.1016/j.foreco.2005.12.011.